

SHORT COMMUNICATION

A NUMERICAL METHOD FOR DIFFUSIVE TRANSPORT WITH MOVING BOUNDARIES AND DISCONTINUOUS MATERIAL PROPERTIES

ZHILIN LI¹, DAVID F. MCTIGUE^{2,*} AND JAN T. HEINE²

¹*Department of Mathematics and Statistics, Mississippi State University, Mississippi State, MS 39762, U.S.A.*

²*Department of Geological Sciences, Box 351310, University of Washington, Seattle, WA 98195, U.S.A.*

SUMMARY

A method for the numerical simulation of diffusive transport with moving boundaries is developed and tested. The variable domain is mapped onto a fixed region, which introduces a term of convective form to the transformed governing equation. The resulting convection/diffusion equation is solved by a finite-difference method. An 'Immersed Interface' Method (IIM) is introduced in order to retain second-order accuracy near discontinuities in material properties, where the solution is not smooth. The method performs well in benchmark calculations against an analytical solution. The IIM scheme is capable of treating a strong discontinuity in the gradient, and it is readily extended to two or three dimensions. The methods are illustrated through a calculation for the temperature profile in a growing continental ice sheet, in which the thermal properties are discontinuous at the rock/ice interface. © 1997 by John Wiley & Sons, Ltd.

Int. J. Numer. Anal. Meth. Geomech., Vol. 21, 653–662 (1997)

(No. of Figures: 3 No. of Tables: 1 No. of Refs: 18)

Key words: moving boundary; parabolic equation; finite difference

INTRODUCTION

Problems that involve diffusive transport of a conserved quantity in a domain with one or more moving boundaries arise frequently in the Earth and environmental sciences. Examples include: the expulsion of water from a growing column of sediment undergoing consolidation (e.g., Reference 1); chemical transport in oceanic sediments undergoing accumulation or erosion at the sea floor (e.g., Reference 2); solidification of magma in an intrusive body (e.g., Reference 3); and heat conduction in a growing ice sheet (e.g., Reference 4). The last of these examples motivated us to consider the moving-boundary problem in some detail, and provides a context for the developments presented here.

Numerical methods for such problems have received much attention.⁵ One challenge is that the boundaries of the computational domain are not fixed in space. In some cases, the location of at least one interface is itself part of the solution. One of a number of artifices must be introduced in

*Correspondence to: D. F. McTigue, 15 Willard Road, New Ipswich, NH 03071, U.S.A.

order to handle the evolution of the domain. For example, one may choose to remesh at each time step in order to retain the same treatment of interfacial conditions throughout a calculation. This approach, of course, introduces considerable complexity, and is computationally intensive. A second numerical challenge arises because material properties are often discontinuous at an interface, so that the solution sought is not smooth. Conventional difference methods introduce error by smoothing out the profile in the neighborhood of an interface.

In this paper, we discuss methods that address each of these difficulties. The moving boundary is handled, in the one-dimensional problems considered, by a 'front-fixing' scheme, in which a change of coordinates fixes the spatial domain, but changes the character of the governing equation. For either this approach or for 'front-tracking' schemes (e.g., Reference 6) that are more easily generalized to two- or three-dimensional domains, error due to the discontinuous gradient at the interface is reduced through an *Immersed Interface Method* (IIM).⁶⁻⁸

DIFFUSIVE TRANSPORT

For present purposes, we consider one-dimensional, diffusive transport of a conserved quantity, although the methods discussed can be applied to a much broader class of problems. Heat conduction provides a generic context for the discussion. It is convenient for the development to state separately the conservation equation:

$$\frac{\partial T}{\partial t} = -\frac{1}{\rho c} \frac{\partial q}{\partial z} \quad (1)$$

and the constitutive model (Fourier's law) for the heat flux, q :

$$q = -k \frac{\partial T}{\partial z} \quad (2)$$

where T is the temperature. The heat capacity, ρc , and thermal conductivity, k , may, in general, vary spatially due to material heterogeneity or due to temperature dependence.

The usual types of boundary conditions, such as specified temperatures and/or fluxes, are stipulated on the ends of the domain. In general, the end boundaries may be moving. In addition, there may be internal, material interfaces at which the properties are discontinuous and jump conditions on the temperature and flux are specified. Such an interface may also move. We consider here, for the sake of illustration, a single moving boundary located at $z = \alpha(t)$, a point that can be on one end of the domain or on an internal interface.

FRONT FIXING

The front-fixing scheme employs a coordinate transformation to map the evolving domain onto a fixed region. Conventional, fixed-grid methods are then directly applicable. Front fixing is a well-established method; a more detailed discussion and historical perspective are provided by Crank.⁹

Consider a domain with a stationary boundary at $z = 0$ and a moving boundary at $z = \alpha(t)$. Define a new co-ordinate

$$\zeta \equiv \frac{z}{\alpha} \quad (3)$$

such that the domain in ζ remains fixed between $\zeta = 0$ and $\zeta = 1$. Equations (1) and (2), written in terms of ζ rather than z , become:

$$\frac{\partial T}{\partial t} = \frac{\zeta}{\alpha} \frac{d\alpha}{dt} \frac{\partial T}{\partial \zeta} - \frac{1}{\rho c} \frac{1}{\alpha} \frac{\partial q}{\partial \zeta} \quad (4)$$

$$q = -\frac{k}{\alpha} \frac{\partial T}{\partial \zeta} \quad (5)$$

One consequence of the transformation is the appearance of a term in the conservation equation (4) of convective form, with ‘effective’ velocity proportional to $-d\alpha/dt$, and varying linearly across the domain. In addition, the heat capacity and conductivity are rescaled by the time-dependent length, α . Thus, the thermal diffusivity, $\kappa \equiv k/\rho c$ in the untransformed problem, is replaced by an ‘effective’ diffusivity, proportional to κ/α^2 in the transformed domain. For a growing region ($d\alpha/dt > 0$), then, the effective diffusivity decreases with time, and the characteristic time scale for the transport correspondingly increases.

NUMERICAL TREATMENT NEAR THE INTERFACE

When we use a difference scheme to discretize equations (1) and (2) or (4) and (5), we lose accuracy near an interface between contrasting materials. This is because the physical properties (here the thermal conductivity and heat capacity) are, in general, discontinuous. We have natural jump conditions on the temperature and the flux:

$$[T] = T(x^+, t) - T(x^-, t) \equiv 0, \quad [q] = \left[-k \frac{\partial T}{\partial x} \right] = -k^+ \frac{\partial T^+}{\partial x} + k^- \frac{\partial T^-}{\partial x} = S(t) \quad (6)$$

across the interface, where $+$ and $-$ stand for the limiting value from the right- and left-hand sides of the interface $x = \alpha(t)$, respectively, and $S(t)$ is the strength of the interfacial source, due, for example, to latent-heat release. We discuss the treatment of the interface in terms of a generic coordinate x in order to emphasize that the method can be applied either to the original problem posed (equations (1) and (2), $x \equiv z$) or to the transformed problem (equations (4) and (5), $x \equiv \zeta$). It is evident that, if $k^+ \neq k^-$, then $T_x^+ \neq T_x^-$ at the interface, i.e., the temperature profile is not smooth. Direct difference discretization will produce large error near the interface when $[k]$ is large or when the net flux $[q]$ is not zero.

A new approach, the IIM,^{7,8} has been developed to solve general PDEs with discontinuous coefficients and/or singular sources with second-order accuracy at all grid points, including those which are close to or on the interface. This approach has also been applied to three-dimensional elliptic equations,¹⁰ parabolic equations,^{6,11} hyperbolic wave equations with discontinuous coefficients,^{12,13} and incompressible Stokes flow problems with moving interfaces.^{14,15} Below we briefly explain this method for our model problem. Readers are referred to Li^{6,8} for a more general treatment of moving-interface problems.

For simplicity in the present development, we assume that the interface is fixed at $x = \alpha$, an interior point in the solution domain, and that the governing equation is linear. Under these conditions, equations (1) and (2) or (3) and (4) can be written

$$\frac{\partial T}{\partial t} = f_1(t) \frac{\partial T}{\partial x} + f_2(t) \frac{\partial^2 T}{\partial x^2} \quad (7)$$

Equation (7) is valid only in the interior of the solution domain. Across an interface, there are jump conditions. In our example problem for a growing ice sheet, we have (6) (with $S \equiv 0$) at the rock/ice interface, and we know the temperature on the surface of the ice sheet, i.e., $T(\alpha, t) = T_0(t)$. We cast our discussion of the IIM in terms of the former type of interface relation.⁴

Assume we use a uniform grid with the spatial step size h , such that $x_i = x_0 + ih$, $i = 0, 1, \dots$, and the interface is between x_j and x_{j+1} , $x_j \leq \alpha < x_{j+1}$. At a regular grid point x_i , $i \neq j, j+1$, the explicit difference scheme can be written as

$$\frac{T_i^{n+1} - T_i^n}{\Delta t} = f_1(t^n) \frac{T_{i+1}^n - T_{i-1}^n}{2h} + f_2(t^n) \frac{T_{i+1}^n - 2T_i^n + T_{i-1}^n}{h^2} \quad (8)$$

where Δt is the time step size. At the irregular grid point x_j , the difference scheme can be written as

$$\frac{T_j^{n+1} - T_j^n}{\Delta t} = \gamma_{j1}^n T_{j-1}^n + \gamma_{j2}^n T_j^n + \gamma_{j3}^n T_{j+1}^n + C_j^n \quad (9)$$

We need to determine the coefficients γ_{j1}^n , γ_{j2}^n , γ_{j3}^n , and the correction term C_j^n so that

$$\begin{aligned} \gamma_{j1}^n T(x_{j-1}, t^n) + \gamma_{j2}^n T(x_j, t^n) + \gamma_{j3}^n T(x_{j+1}, t^n) + C_j^n \\ \approx (f_1(t^n) T_x + f_2(t^n) T_{xx})_{(\alpha, t^n)} \end{aligned} \quad (10)$$

The idea is simple; we expand $T(x_{j-1}, t^n)$ and $T(x_j, t^n)$ in Taylor series about α from the left, and $T(x_{j+1}, t^n)$ from the right of α . Then the left-hand side of (10) becomes

$$\begin{aligned} \gamma_{j1}^n \left(T^- + T_x^- (x_{j-1} - \alpha) + T_{xx}^- \frac{(x_{j-1} - \alpha)^2}{2} \right) + \gamma_{j2}^n \left(T^- + T_x^- (x_j - \alpha) + T_{xx}^- \frac{(x_j - \alpha)^2}{2} \right) \\ + \gamma_{j3}^n \left(T^+ + T_x^+ (x_{j+1} - \alpha) + T_{xx}^+ \frac{(x_{j+1} - \alpha)^2}{2} \right) + C_j^n + \dots \end{aligned} \quad (11)$$

where all quantities are calculated at (α, t^n) . From the interface relations (6), we have

$$T^+ = T^-, \quad T_x^+ = \frac{k^- T_x^- - S}{k^+} \quad (12)$$

Also from the differential equation (7), we have

$$f_1^+ T_x^+ + f_2^+ T_{xx}^+ = f_1^- T_x^- + f_2^- T_{xx}^- \quad (13)$$

Here we have used the assumption that $T(x, t)$ is continuous and the interface α is fixed. From (12)–(13) we obtain

$$T_{xx}^+ = \frac{f_2^-}{f_2^+} T_{xx}^- + \frac{f_1^-}{f_2^+} T_x^- + \frac{f_1^+ S - k^- T_x^-}{f_2^+ k^+} \quad (14)$$

Substituting (12) and (14) into (11) and arranging terms we have

$$(\gamma_{j1}^n + \gamma_{j2}^n + \gamma_{j3}^n) T^- + \left\{ \gamma_{j1}^n (x_{j-1} - \alpha) + \gamma_{j2}^n (x_j - \alpha) + \gamma_{j3}^n \left(\frac{k^-}{k^+} (x_{j+1} - \alpha) \right. \right.$$

$$\begin{aligned}
& + \left(\frac{f_1^-}{f_2^+} - \frac{k^- f_1^+}{k^+ f_2^+} \right) \frac{(x_{j+1} - \alpha)^2}{2} \Bigg\} T_x^- + \left(\gamma_{j1}^n \frac{(x_{j-1} - \alpha)^2}{2} + \gamma_{j2}^n \frac{(x_j - \alpha)^2}{2} \right. \\
& \left. + \gamma_{j3}^n \frac{f_2^-}{f_2^+} \frac{(x_{j+1} - \alpha)^2}{2} \right) T_{xx}^- - \gamma_{j3}^n S \left(\frac{(x_{j+1} - \alpha)}{k^+} - \frac{f_1^+}{f_2^+} \frac{(x_{j+1} - \alpha)^2}{2} \right) + C_j^n + \dots \quad (15)
\end{aligned}$$

Comparing (15) with the right-hand side of (10), we obtain three equations for γ_{j1}^n , γ_{j2}^n , and γ_{j3}^n as follows:

$$\gamma_{j1}^n + \gamma_{j2}^n + \gamma_{j3}^n = 0 \quad (16)$$

$$\gamma_{j1}^n (x_{j-1} - \alpha) + \gamma_{j2}^n (x_j - \alpha) + \gamma_{j3}^n \left\{ \frac{k^-}{k^+} (x_{j+1} - \alpha) + \left(\frac{f_1^-}{f_2^+} - \frac{k^- f_1^+}{k^+ f_2^+} \right) \frac{(x_{j+1} - \alpha)^2}{2} \right\} = f_1(t^n) \quad (17)$$

$$\gamma_{j1}^n \frac{(x_{j-1} - \alpha)^2}{2} + \gamma_{j2}^n \frac{(x_j - \alpha)^2}{2} + \gamma_{j3}^n \frac{f_2^-}{f_2^+} \frac{(x_{j+1} - \alpha)^2}{2} = f_2(t^n) \quad (18)$$

and the correction term is determined as

$$C_j^n = \gamma_{j3}^n S \left(\frac{(x_{j+1} - \alpha)}{k^+} - \frac{f_1^+}{f_2^+} \frac{(x_{j+1} - \alpha)^2}{2} \right) \quad (19)$$

which is known after γ_{j3}^n is obtained from (16)–(18). If $S(t) = 0$, as in our model problem for the ice sheet, then $C_j^n = 0$. Similarly, we can derive the modified difference scheme at the regular grid point x_{j+1} .

IMPLEMENTATION: METHOD OF LINES

The development of the IIM was outlined in the previous section in the context of the linear PDE given by (7), and in difference form by (8) and (9). In a more general treatment allowing for continuously varying, temperature-dependent properties, we discretize (4) at regular grid points in the form:

$$\frac{T_i^{n+1} - T_i^n}{\Delta t} = \frac{\zeta_i}{\alpha} \frac{d\alpha}{dt} \frac{T_{i+1}^n - T_{i-1}^n}{2h} - \frac{1}{(\rho c)_i} \frac{1}{\alpha} \frac{q_{i+1/2}^n - q_{i-1/2}^n}{h} \quad (20)$$

where α and $d\alpha/dt$ are evaluated at t^n , and the fluxes (5) are evaluated at mid-point nodes corresponding to $\zeta_i \pm \frac{1}{2}h$:

$$q_{i+1/2} = - \frac{k_{i+1/2}}{\alpha} \frac{T_{i+1} - T_i}{h}, \quad q_{i-1/2} = - \frac{k_{i-1/2}}{\alpha} \frac{T_i - T_{i-1}}{h} \quad (21)$$

with all quantities in (21) evaluated at time t^n . For irregular grid points, adjacent to interfaces across which the gradient is discontinuous, we implement the IIM, modified to account for the nonlinearity in the two contrasting materials.

The temperatures are computed for grid points, while, from (21), we must compute the temperature-dependent conductivity at the midpoints. We invoke the following approximation:¹⁶

$$k_{i+1/2} = \frac{2k_i k_{i+1}}{k_i + k_{i+1}}, \quad k_{i-1/2} = \frac{2k_{i-1} k_i}{k_{i-1} + k_i} \quad (22)$$

where, for example, the conductivity k_i is computed from the temperature T_i^n . The weightings given in (22) are constructed by matching the heat fluxes at the midpoints, which are approximated by backward and forward differences over the adjacent half-intervals. In the special case of piecewise-constant properties, equations (20)–(22) reduce to the form of (8).

We call the SLATEC backward-difference solver DEBDF¹⁷ to perform the time integration. This is a variable-order, variable-step routine that utilizes a Newton-type algorithm to solve the system of coupled, nonlinear, algebraic equations for the nodal temperatures given by (20)–(22).

BENCHMARK PROBLEM

In order to test the solution scheme, we construct a relatively difficult numerical problem having an analytical solution. We consider two materials, separated by a moving interface. The material properties are assumed to be piecewise constant. However, we consider an arbitrary contrast in the conductivity, k , across the material interface, implying that the temperature gradient may be strongly discontinuous (differing by the ratio of the conductivities, cf. the second jump condition given in (6)).

We consider a finite domain, $0 \leq z \leq L$, in the interior of which is a moving interface located at $z = \alpha(t)$. Denote the domain $0 \leq z < \alpha$ the ‘minus’ (–) region, and $\alpha < z \leq L$ the ‘plus’ (+) region, with material properties for each region correspondingly designated, e.g., k^- and k^+ . The interface is assumed to be located at

$$z = \alpha = 2\sqrt{\kappa^- t} \quad (23)$$

A solution satisfying (1) and (2), as well as satisfying continuous temperature and heat flux at the interface $z = \alpha$, is

$$T = \begin{cases} 1 - \frac{\text{erf}(\eta)}{\text{erf}(1)}, & 0 \leq z \leq \alpha \\ C \left[1 - \frac{\text{erf}(R\eta)}{\text{erf}(R)} \right], & \alpha \leq z \leq L \end{cases} \quad (24)$$

where $\eta \equiv z/2\sqrt{\kappa^- t}$, $C \equiv \beta R \exp(R^2 - 1) \text{erf}(R)/\text{erf}(1)$, $\beta \equiv (\rho c)^-/(\rho c)^+$, and $R^2 \equiv \kappa^-/\kappa^+$. This solution satisfies the Dirichlet conditions at $z = 0$ and $z = L$:

$$T(0, t) = 1, \quad T(L, t) = C \left[1 - \frac{\text{erf}(L/2\sqrt{\kappa^+ t})}{\text{erf}(R)} \right] \quad (25)$$

In this example, we solve the problem with the front-fixing scheme. With reference to (7), $x \equiv \zeta$, $f_1 \equiv (\zeta/\alpha) d\alpha/dt$, and $f_2 \equiv \kappa/\alpha^2$, the rescaled thermal diffusivity, is piecewise constant at any particular time.

We compare our method with a conventional approach in discretizing the diffusion term κT_{zz} , the *smoothing method*. Here, we solve the untransformed problem, so that in (7), $x \equiv z$, $f_1 \equiv 0$, and $f_2 \equiv \kappa$, where, again, the diffusivity is piecewise constant. The smoothing method is defined

as follows:

$$\tilde{k} = \begin{cases} k^- & \text{if } z < \alpha - \varepsilon \\ \frac{k^- + k^+}{2} + \frac{k^+ - k^-}{2} \sin \frac{(z - \alpha)\pi}{2\varepsilon} & \text{if } |z - \alpha| \leq \varepsilon \\ k^+ & \text{if } z > \alpha + \varepsilon \end{cases} \quad (26)$$

The smoothing method is only first-order accurate and is difficult to extend to two dimensions. If we let ε approach zero, then the conductivity takes its exact value everywhere except at the interface, $z = \alpha$, where it is represented by the average: $\tilde{k} = (k^- + k^+)/2$. This approach is crude, but simple and widely used. One advantage is that it can be used in two-dimensional problems. It usually gives less accurate results than the smoothing method. A more subtle discretization is obtained by harmonic averaging; see Li⁸ for a detailed discussion.

Table I shows a comparison of the error in the computed solution in the infinity norm defined as

$$\|E_N\|_\infty = \max_i |T(z_i, t_{\text{out}}) - T_i^{n^*}| \quad (27)$$

where n^* is the final time step corresponding to the time t_{out} . The parameters are: $t_0 = 0.5$, $t_{\text{out}} = 0.6$, $\beta = 1$, $R^2 = 0.05$, where the initial condition, at $t = t_0$, is computed from the exact solution. We take $(\rho c)^- = (\rho c)^+ = 1$, and $k^- = 1$, $k^+ = 20$ in order to consider the twenty-fold contrast in the diffusivity indicated at the interface. We see that our method, the IIM, gives a much better result (Figure 1).

Table I. Comparison of the IIM with the smoothing method. N is the number of grid points

N	$\ E_N\ _\infty$, IIM	$\ E_N\ _\infty$, Smoothing
80	5.10×10^{-5}	7.32×10^{-3}
160	2.00×10^{-5}	9.18×10^{-4}
320	2.98×10^{-6}	6.77×10^{-4}

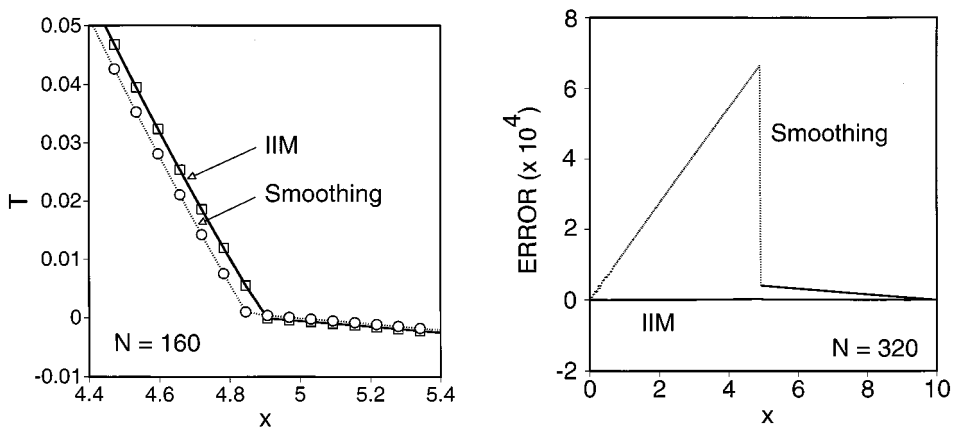


Figure 1. (a) Local solution plot. The result obtained with the IIM is so close to the exact solution that they appear identical on this plot. $N = 160$. (b) Error plot (cf. (27)) for the IIM and the smoothing method. $N = 320$

EXAMPLE: THERMAL EVOLUTION IN A GROWING ICE SHEET

We use the model described to simulate the temperature profile at the centre of an ice sheet throughout the course of a glaciation. The base of an ice sheet is either frozen to its bed ('cold-based'), or at the pressure melting point ('warm-based'). An ice sheet becomes warm-based when the geothermal heat flux and internal heating by viscous dissipation provide enough heat to melt the base of the ice sheet, while the overlying ice mass insulates the base against the very cold air at the surface.¹⁸ Determination of the basal conditions of ice sheets is of paramount importance for the reconstruction of their topography and flow characteristics. Slip at the bed of a warm-based ice sheet results in far greater erosion than that produced by ice frozen to the substrate. We consider the centre of the ice sheet, where horizontal flow vanishes and the heat transfer may be approximated by a one-dimensional model.

The model accounts for conduction in both the ice and the underlying rock. In previous calculations,⁴ we have considered temperature-dependent thermal conductivity and heat capacity for the ice. However, this introduces only a weak non-linearity that has minimal influence on the final results. Here, we restrict our sample calculation to the linear problem for piecewise constant properties. At the start of a model run, subsurface temperatures are in equilibrium with the geothermal heat flux and a given ground surface temperature. The geothermal heat flux is applied at a depth of 4000 m, which was found, in the present context, to be effectively an infinite boundary. Ice is deposited on the surface at the surface temperature. Ice sheet growth is defined by, $\alpha/\alpha_\infty = 1 - \exp(-t/t_r)$. The rise time, t_r , is 6000 years, and the final ice sheet thickness, α_∞ , is 3000 m. The surface temperature is held constant at -20°C . The calculation is stopped when basal melting occurs at about -2°C , the melting point at a pressure corresponding to 3000 m of ice. We neglect latent heat released by the melting of ice contained within the near-surface rock because we are concerned primarily with crystalline rock with very small porosity. However, we note that the methods described here are well suited to treatment of the moving phase-change boundary, or Stefan problem.

Figure 2 displays the temperature profile within the ice/rock body at various times. The basal melting point is reached after 64,000 years (Figure 3). For a more detailed description of the ice sheet model including the effects of temperature-dependent thermal properties, vertical advection due to accumulation and divergent, horizontal flow, and adiabatic cooling of the surface, see Heine and McTigue.⁴ Although this simple model neglects several processes that affect the thermal regime in an ice sheet, the qualitative result is significant. Because the thermal diffusion time, α_∞^2/κ , and the time scale for a typical glacial cycle are both of the order of 10^5 years, the transient evolution of the temperature profile must be considered. In the past, some models have assumed a steady-state thermal balance. For reasonable surface temperature and sufficiently thick ice this inevitably leads to the conclusion that the ice sheet is warm-based. However, the transient model discussed here suggests that the time required for the base of the ice sheet to approach its steady-state temperature is so long that the center of the ice sheet remains cold-based, at least through a large portion of a glacial cycle. This conclusion is consistent with emerging geomorphologic evidence of relatively little glacial erosion under past continental ice sheets.

We note that, in the problem considered here, the conductivity contrast at the rock/ice interface is small: $k^-/k^+ = 1.09$. Thus, conventional methods that result in some smoothing of the temperature profile near the interface may be satisfactory in this context. However, the IIM is of increasing utility as the contrast in material properties increases, as demonstrated in the benchmark problem treated in the preceding section.

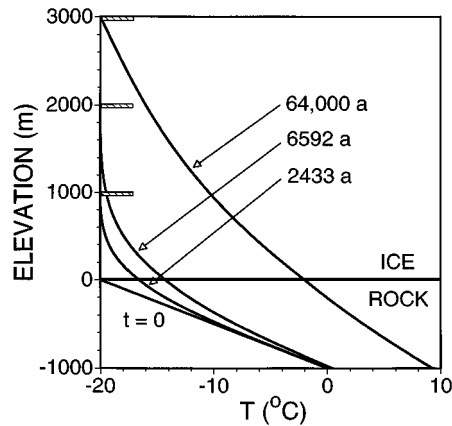


Figure 2. Temperature profiles through the ice sheet at times corresponding to 1000 m increments of growth. Final profile is for 64,000 years, when the interface reaches the melting point (-2°C). The thermal properties are discontinuous at the rock/ice interface, at elevation = 0. Rock: $k^- = 2.5 \text{ W/m/K}$, $(\rho c)^- = 2.3 \times 10^6 \text{ J/m}^3/\text{K}$. Ice: $k^+ = 2.3 \text{ W/m/K}$ and $(\rho c)^+ = 1.8 \times 10^6 \text{ J/m}^3/\text{K}$. Far-field geothermal flux is 0.05 W/m^2

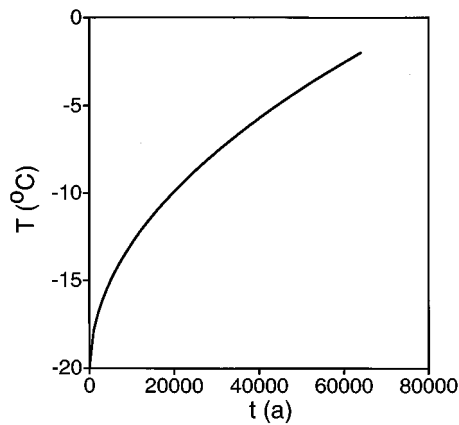


Figure 3. Temperature rise at the rock/ice interface. The melting point, -2°C for an overburden of 3000 m of ice, is reached after 64,000 years

CONCLUSION

A front-fixing scheme and an Immersed Interface Method (IIM) have allowed us to solve a class of problems involving moving boundaries and discontinuous material properties with second-order accuracy throughout the domain. The front-fixing approach is quite straightforward in one dimension, but is considerably more difficult to implement for multidimensional domains. In contrast, the IIM can be embedded in any number of schemes for treating the moving interface, and therefore is readily adapted to two- or three-dimensional calculations. The accuracy maintained by the IIM in the neighbourhood of a strong discontinuity in conductivity (or, equivalently, in the temperature gradient) is demonstrated in a benchmark comparison to an analytical

solution. Finally, the methods prove to be quite successful in simulating the evolution of the thermal profile through an accumulating continental ice sheet. In this application, the temperature history at the material discontinuity is the central issue, and accuracy near the interface is of particular importance.

ACKNOWLEDGEMENT

We are grateful to M. R. Baer for extensive discussion of the numerical analysis.

REFERENCES

1. R. E. Gibson, 'The progress of consolidation in a clay layer increasing in thickness with time', *Geotechnique*, **8**, 171–182 (1958).
2. A. Lerman and T. A. Lietzke, 'Fluxes in a growing sediment layer', *Am. J. Sci.*, **277**, 25–37 (1977).
3. P. T. Delaney and D. D. Pollard, 'Solidification of basaltic magma during flow in a dike', *Am. J. Sci.* **282**, 856–885 (1982).
4. J. T. Heine and D. F. McTigue, 'A case for cold-based continental ice sheets—a transient thermal model', *J. Glaciology*, **42**, 37–42 (1996).
5. M. Zerroukat and C. R. Chatwin, *Computational Moving Boundary Problems*, Wiley, New York, 1994, 222 pp.
6. Z. Li, 'Immersed interface method for moving interface problems', *Numerical Algorithms* (1996) in press; *UCLA CAM Report #95-25*.
7. R. J. LeVeque and Z. Li, 'The immersed interface method for elliptic equations with discontinuous coefficients and singular sources', *SIAM J. Numer. Anal.*, **31**, 1019–1044 (1994).
8. Z. Li, *The Immersed Interface Method — A Numerical Approach for Partial Differential Equations with Interfaces*, Ph.D. thesis, University of Washington, 1994.
9. J. Crank, *Free and Moving Boundary Problems*, Clarendon, Oxford, 1984, pp. 163–186.
10. Z. Li, 'A note on immersed interface methods for three dimensional elliptic equations', *Comput. Math. Appl.*, **31**, 9–17 (1996).
11. Z. Li and A. Mayo, 'ADI methods for heat equations with discontinuities along an arbitrary interface', in W. Gautschi (ed.), *Proc. Symp. on Applied Mathematics*, Vol. **48**, American Mathematical Society, Providence, RI, 1993.
12. C. Zhang and R. J. LeVeque, 'Immersed interface methods for wave equations with discontinuous coefficients', *Wave Motion*, 1996, in press.
13. R. J. LeVeque and C. Zhang, 'Finite difference methods for wave equations with discontinuous coefficients', *Proc. ASCE Conf.*, S. Sture (ed.), (1995), in press.
14. R. J. LeVeque and Z. Li, 'Simulation of bubbles in creeping flow using the immersed interface method', *Proc. 6th Internat. Symp. on Computational Fluid Dynamics*, 1995, pp. 688–693.
15. R. J. LeVeque and Z. Li, 'Immersed interface method for Stokes flow with elastic boundaries or surface tension', *Technical Report #95-01*, University of Washington, also *SIAM J. Scientific Statistical Comput.* 1995, in press.
16. R. J. Gross, M. R. Baer and M. L. Hobbs, 'XCHEM-1D: A heat transfer/chemical kinetics computer program for multilayered reactive materials', *Sandia National Laboratories Technical Report*, **SAND93-1603**, Albuquerque, New Mexico, 1993.
17. L. F. Shampine and H. A. Watts, 'DEPAC — Design of a user oriented package of ODE solvers', *Sandia National Laboratories Technical Report*, **SAND79-2374**, Albuquerque, New Mexico, 1980.
18. W. S. B. Paterson, *The Physics of Glaciers*, 3rd edn, Pergamon, Oxford, 1994, 480 pp.